Biogeosciences

Saturated CO_2 inhibits microbial processes in CO_2-vented deep-sea sediments

D. de Beer[1], **M. Haeckel**[2], **J. Neumann**[1], **G. Wegener**[1,3], **F. Inagaki**[4,5], **and A. Boetius**[1,6]

[1]Max Planck Institute for Marine Microbiology, Celsiusstrasse 1, 28359 Bremen, Germany
[2]Geomar Helmholtz Centre for Ocean Research Kiel, Wischhofstrasse 1–3, 24148 Kiel, Germany
[3]MARUM – Center for Marine Environmental Sciences, University of Bremen, 28334 Bremen, Germany
[4]Geomicrobiology Group, Kochi Institute for Core Sample Research, Japan Agency for Marine-Earth Science and Technology (JAMSTEC), Monobe B200, Nankoku, Kochi 783-8502, Japan
[5]Geobio-Engineering and Technology Group, Submarine Resources Research Project, JAMSTEC, Monobe B200, Nankoku, Kochi 783-8502, Japan
[6]HGF MPG Research Group for Deep Sea Ecology and Technology, Alfred Wegener Institute for Polar and Marine Research, Am Handelshafen, 27515 Bremerhaven, Germany

Correspondence to: D. de Beer (dbeer@mpi-bremen.de)

Abstract. This study focused on biogeochemical processes and microbial activity in sediments of a natural deep-sea CO_2 seepage area (Yonaguni Knoll IV hydrothermal system, Japan). The aim was to assess the influence of the geochemical conditions occurring in highly acidic and CO_2 saturated sediments on sulfate reduction (SR) and anaerobic methane oxidation (AOM). Porewater chemistry was investigated from retrieved sediment cores and in situ by microsensor profiling. The sites sampled around a sediment-hosted hydrothermal CO_2 vent were very heterogeneous in porewater chemistry, indicating a complex leakage pattern. Near the vents, droplets of liquid CO_2 were observed emanating from the sediments, and the pH reached approximately 4.5 in a sediment depth > 6 cm, as determined in situ by microsensors. Methane and sulfate co-occurred in most sediment samples from the vicinity of the vents down to a depth of 3 m. However, SR and AOM were restricted to the upper 7–15 cm below seafloor, although neither temperature, low pH, nor the availability of methane and sulfate could be limiting microbial activity. We argue that the extremely high subsurface concentrations of dissolved CO_2 (1000–1700 mM), which disrupt the cellular pH homeostasis, and lead to end-product inhibition. This limits life to the surface sediment horizons above the liquid CO_2 phase, where less extreme conditions prevail. Our results may have to be taken into consideration in assessing the consequences of deep-sea CO_2 sequestration on benthic element cycling and on the local ecosystem state.

1 Introduction

The increase in atmospheric CO_2 will lead to global warming and acidification of the ocean. One of the possible countermeasures considered is to separate CO_2 from waste gas of large production units, such as power plants and cement ovens, and to pump it in liquefied form into the deep seafloor. Depending on in situ pressure and temperature, it will become gas hydrate, liquid or supercritical, and may be sequestered during the weathering of sedimentary carbonates and silicates (House et al., 2006; IPCC, 2007; Wallmann et al., 2008). This process of carbon dioxide capture and storage (CCS) would not bind CO_2 as such, but lead to neutralization of the acidified seawater. Besides economic costs and safety aspects, the risks of such activities for biodiversity and element cycling in the deep sea are to be considered (Seibel and Walsh, 2001). Here we focused on the long-term effects of high CO_2 and low pH on biogeochemical processes in deep-sea sediments of a natural CO_2-venting hydrothermal system. CO_2 emitted from hydrothermal sediments can be considered as a natural analogue of the CO_2 leakage associated

with CCS in the deep-sea floor under realistic environmental conditions and scales. Experimental studies of the interaction of liquid CO_2 with microorganisms and geochemical processes in deep-sea sediments remain challenging, because of the high pressure and steep gradients associated with point sources of CO_2 (Liu et al., 2010).

A main question for CCS risk assessment is as to the effect of high CO_2 emissions on the functioning of marine ecosystems. Numerous studies of seafloor microbial ecology and biogeochemistry have demonstrated that microbial processes dominate the biogeochemistry of deep-sea sediments (Jørgensen and Boetius, 2007; Jørgensen and Nelson, 2004; Reeburgh, 1983). When not limited by thermodynamics or transport, their function may be limited by kinetics due to physicochemical conditions in the habitat. Microbial metabolic activity can be inhibited and kinetics can be changed by toxic compounds (e.g. strong oxidants, heavy metals, uncouplers of membrane potentials). High temperatures ($> 122\,^{\circ}\mathrm{C}$) can also degrade enzymatic function. However, highly adapted microorganisms have been found to populate environments with extremes in pH values, pressure, salinity, and radiation levels. Thus, these parameters do not limit life in general (Stan-Lotter and Fendrihan, 2012); in other words, life has shown to be remarkably adaptive to a very wide range of conditions. Yet it remains unknown if main ecosystem functions such as aerobic and anaerobic remineralization and respiration of matter, autotrophy, and methane oxidation can be maintained under extremely high CO_2 levels, as will occur at CCS sites in the deep-sea floor. Here we tested the hypothesis that the main biogeochemical processes mediated by microorganisms can function in CO_2 saturated porewater of deep-sea sediments.

The occurrence of liquid CO_2 in a natural marine setting has been firstly observed in the Jade hydrothermal field, Okinawa Trough (Sakai et al., 1990), and was subsequently found also at other hydrothermal systems at water depths between 1200 and 1700 m, such as the NW Eifuku hydrothermal field in the Mariana Arc and the Yonaguni Knoll IV hydrothermal system in the Okinawa Trough. The Yonaguni Knolls are submarine volcanoes located in the southwestern end of the Okinawa Trough (Suzuki et al., 2008). The Yonaguni Knoll IV hydrothermal system is one of the few sites on earth known where liquid CO_2 leaks through thick layers of terrigenous sediments supplied from the Asian continent (Sibuet et al., 1987). It comprises a sedimentary valley surrounded by large piles of rock debris, enclosing a string of active hydrothermal vents. A previous characterization of the hydrothermal fluids indicated the generation of liquid CO_2 by subsurface phase separation (Konno et al., 2006; Suzuki et al., 2008). Besides their high CO_2 content, the hydrothermal fluids exhibit a wide variation in gas composition including H_2, CH_4, H_2S and NH_3. Previous studies have focussed on the distribution of bacterial and archaeal communities of the Yonaguni Knoll IV hydrothermal sediments and overlying bottom waters (Inagaki et al., 2006; Yanagawa et al., 2012;

Nunoura et al., 2010). Here we have investigated the biogeochemistry of the CO_2 vented sediments, focussing on the distribution of microbial aerobic and anaerobic respiration pathways. Combining in situ and ex situ analytical techniques, we investigated rates of benthic oxygen consumption, sulfate reduction (SR) and anaerobic oxidation of methane (AOM) to cover the ecologically important biogeochemical processes in the CO_2-impacted system. These data form the basis for a discussion of the effects of low pH and high CO_2 conditions on the functioning of deep-sea ecosystems to be considered in the risk assessment of offshore geological CCS.

2 Methods

2.1 Sampling location and methods

Samples were taken in February–March 2008 during the RV *Sonne* 196 expedition with ROV *QUEST* in the project SUM-SUN ("Studies of marine CO_2 sequestration associated with a natural hydrothermal CO_2 system of the northern west Pacific") (Rehder and Schneider von Deimling, 2008). The area was revisited for a few additional samples during the JAM-STEC NT10-06 Leg 3 cruise with RV *Natsushima* and ROV *Hyper Dolphin* in April 2010.

The Yonaguni Knoll IV hydrothermal field is located in the Okinawa Trough ($24°50.7'$ N, $122°42.0'$ E; 1320–1399 m water depths) (Table 1). The hydrothermal system is part of a sedimentary basin covered by volcanic rocks in its northeastern part, hosting several large hydrothermal vent chimneys (Konno et al., 2006; Suzuki et al., 2008). A sedimentary venting site characterized by a few holes in the seafloor emitting hot fluids was discovered on the southern end of the hydrothermal field and named "Abyss Vent" (Inagaki et al., 2006). In situ measurements were carried out along a transect from Abyss Vent (i.e. < 1 m, 10 m, 100 m, 125 m distance), as well as in sediments near "Swallow Chimney" vent, ~ 100 m north of the Abyss Vent and a sedimentary site 0.5 km southwest of the hydrothermal system for non-CO_2 impacted reference samples. Sediment samples from the uppermost sediment horizons (top 20–30 cm) were taken either with a video-guided multiple corer (MUC, 10 cm diameter cores), with push cores (PCs, 8 cm diameter cores) collected with the manipulator of the ROV, or with gravity cores (GC, 10 cm diameter, up to 3 m sediment depth). All sampling instruments were equipped with a POSIDONIA (Ixsea SAS) positioning system for targeted geo-referenced seafloor sampling. After recovery, the sediment samples were transferred to a cold room that was cooled to near in situ temperature ($4\,^{\circ}\mathrm{C}$). Subsequently, the cores were vertically subsampled with small subcore tubes for activity rate analyses and porewater extraction as described below.

Table 1. Station list with sampling dates and locations.

Cruise name	Device type	No.	Date	N	E	Depth (m)
SO196	MP	D201,1	13.03.2008	24 50.781	122 42.0307	1382
SO196	MP	D201,2	13.03.2008	24 50.782	122 42.0251	1381
SO196	MP	D201,3	13.03.2008	24 50.826	122 42.0842	1365
SO196	PC	D201,1	13.03.2008	24 50.781	122 42.0273	1382
SO196	PC	D201,5	13.03.2008	24 50.781	122 42.0273	1382
SO196	PC	D201,21	13.03.2008	24 50.781	122 42.0273	1382
SO196	PC	D201,23	13.03.2008	24 50.781	122 42.0273	1382
SO196	PC	D203,11	16.03.2008	24 50.783	122 42.0347	1380
SO196	PC	D203,14	16.03.2008	24 50.783	122 42.0360	1380
SO196	PC	D203,24	16.03.2008	24 50.780	122 42.0285	1383
SO196	PC	D203,29	16.03.2008	24 50.784	122 42.0365	1380
SO196	PC	D203,33	16.03.2008	24 50.782	122 42.0290	1383
SO196	MUC	3	08.03.2008	24 50.827	122 42.086	1372
SO196	MUC	8	08.03.2008	24 50.838	122 41.992	1362
SO196	MUC	10	09.03.2008	24 50.791	122 42.020	1392
SO196	MUC	23	17.03.2008	24 50.355	122 41.736	1324
SO196	MUC	28	21.03.2008	24 50.781	122 42.028	1394
SO196	GC	1	12.03.2008	24 50.841	122 42.003	1382
SO196	GC	3	15.03.2008	24 50.851	122 42.019	1383
SO196	GC	8	20.03.2008	24 50.341	122 41.726	1320
SO196	GC	9	20.03.2008	24 50.774	122 42.043	1399
SO196	BC	D203, 1	16.03.2008	24 50.783	122 42.0303	1380
SO196	BC	D203, 2	16.03.2008	24 50.781	122 42.0266	1382
SO196	BC	D206, 1	21.03.2008	24 50.479	122 41.8599	1347
SO196	BC	D206, 2	21.03.2008	24 50.776	122 42.0383	1381
NT10_06	MP	1	17.04.2010	24 50.515	122 41.882	1355
NT10_06	MP	2	17.04.2010	24 50.784	122 42.099	1387
NT10_06	PC	1	17.04.2010	24 50.515	122 41.882	1355

MP = microprofiler, PC = push core, MUC = multicore, GC = gravity core, BC = benthic chamber, D = *QUEST* Dive No.

2.2 Porewater extraction and chemical analyses

Porewater was extracted using a low-pressure squeezer (argon at 1–5 bar) at approximately in situ temperature of 4 °C in the ship's cold room. While squeezing, the porewater was filtered through 0.2 µm polycarbonate Nuclepore filters and collected in vials. Onboard, the collected porewater samples were analyzed for their content of dissolved NH_4^+, H_2S, and SiO_4^{4-} using standard photometric methods (Grasshoff et al., 1999), and total alkalinity (TA) by titration with 0.01 N HCl against an indicator mixture consisting of methyl red and methylene blue. In addition, subsamples were taken and stored at 4 °C for shore-based analysis of SO_4^{2-} using ion chromatography. Porosity was determined from 5 mL of wet sediment by freeze-drying and weight difference assuming a sediment density of 2.5 g cm^{-3} and a porewater density of 1.023 g cm^{-3}. An additional 3 mL of sediment was suspended in 9 mL of 0.1 N NaOH in a 20 mL vial for methane headspace analysis. Methane was measured using a standard gas chromatograph using a flame ionization detector.

2.3 Microprofiling

Microsensors for O_2, H_2S, and pH were made and used as described previously (de Beer et al., 1997; Jeroschewski et al., 1996; Revsbech, 1989). The tip diameters were approximately 20 µm, the response time (t_{90}) less than 3 s. A temperature sensor was used (Pt100, UST Umweltsensortechnik GmbH, Thüringen, Germany), with a length of 18 cm, a shaft and tip diameter of 3 mm and length of sensing element of 1 cm and a response time of ∼ 5 s. Microsensors for redox potential (ORP) were made from Pt wire of 50 µm diameter, fused in a glass capillary, leaving a length of 100 µm Pt exposed as sensing surface. After mounting, the Pt tip was cleaned in 6 M HNO$_3$ for 10 min, and rinsed with distilled water before calibration in standard redox buffers. All sensors were calibrated after mounting on the profiler. The sensors were mounted on the bottom of the titanium housing within a distance of maximally 11 cm. The titanium housing, containing amplifiers and a computer for data acquisition and motor control, could be moved vertically by a high precision motor. The profiler was preprogrammed to measure vertical

profiles, with steps of 250 µm, over a depth of 17 cm. The profiler was positioned at the seafloor by a ROV and started by a switch on the profiler. After finishing a profile, the profiler could be repositioned and restarted.

The slope of the pH calibration was taken, as during the calibration the pressure induced offset was corrected for with the pH determined from Niskin bottle samples from 50 cm above the sediment surface. The O_2 sensors were 2-point calibrated in situ, by using the signal in the bottom water and in the anoxic zones of the sediments. The bottom water O_2 concentration was measured by Winkler titration from the same Niskin bottles. Total sulfide was calculated from the local pH and H_2S concentrations, using a pK value for sulfide of 6.92, as calculated from the local temperature and salinity (Millero et al., 1988). The H_2S sensors had detection limits for H_2S of $1 \mu mol \, L^{-1}$. For profile analysis, the surface was taken as the reference point (depth = 0), defined by the steepest slope of the oxygen profile (Gundersen and Jørgensen, 1990). Negative depths indicate positions above the sediment surface.

2.4 Benthic chamber measurements

Methane, dissolved inorganic carbon (DIC), and ammonium fluxes were determined with a cylindrical benthic chamber module as previously described (Felden et al., 2010) operated by the ROV *QUEST*. Briefly, the stirred chamber (radius 9.5 cm) enclosed a seafloor area of $284 \, cm^2$ together with 10–15 cm (equivalent to 4–6 L) of overlying bottom water. A valve in the chamber lid ensured the release of overpressure while placing the chamber gently into the sediment. Five water samples were taken with 50 mL syringes at pre-programmed time intervals to determine the fluxes of dissolved methane, silicate and ammonium. All chemical analyses followed standard procedures (Grasshoff et al., 1999). The fluxes were calculated from the linear regressions of concentration vs. time over the area of the sediment enclosed by the chamber.

2.5 Methane oxidation and sulfate reduction rates

Sediment cores for measurements of anaerobic oxidation of methane and sulfate reduction were subsampled on board with three replicates per sample site. The rates were measured according to previously published protocols (Treude et al., 2005). Briefly, either 25 µL $^{14}CH_4$ (dissolved in water, 2.5 kBq) or 5–10 µL carrier-free $^{35}SO_4^{2-}$ (dissolved in water, 50 kBq) were injected in 1 cm intervals into the subcores. The sediment was incubated in the dark at in situ temperature for 12–48 h. After the incubation, the reaction was terminated by cutting 1 cm sections of the sediment cores into the respective fixative for further analysis in the home laboratory.

3 Results

3.1 Visual observations

The Yonaguni Knoll IV study area comprises an approximately 1 nautical-mile-wide sedimentary valley surrounded by rocky slopes in the west and northeast. A number of hydrothermal chimneys are located roughly on a line in the NW–SE-direction (Fig. 1). In addition to the mineral chimneys through which hot fluids > 300 °C escape, we observed pavements of elemental sulfur and amorphous SiO_2 precipitates associated with holes and cracks in the underlying soft sediments from which hot fluids and liquid CO_2 emanated. The seafloor area surrounding the vents and sulfur pavements lacked bottom-dwelling megafauna and showed no typical features of bioturbation, burrows or other traces of life. Only on active chimneys was dense accumulation of chemosynthetic fauna observed, including the mussel *Bathymodiolus platifrons*, the shrimp *Alvinocaris longirostris*, and the crab *Shinkaia crosnieri*. No mats of giant sulfide-oxidizing bacteria typical for sulfide-emitting hydrothermal vents and hydrocarbon seeps were observed on the rocks or the seafloor. The sedimentary seafloor was flat and featureless; i.e. there were no pockmarks or ebullition holes away from the vents.

In the absence of morphological indications for subseafloor CO_2 leakage, our sampling strategy was to sample the sediments in the immediate vicinity of active CO_2-emitting vents, such as the Abyss Vent and the Swallow Chimney vent. When push cores were pulled out of the vented sediments by the ROV arm, liquid CO_2 droplets escaped from the sampling hole. This phenomenon was restricted to the < 20 m vicinity of the vents. Abyss Vent was marked by a couple of round openings of 10 cm diameter from which hot CO_2-rich water (> 60 °C) was ejected. Swallow Chimney was surrounded by sulfur pavements and emitted relatively cold fluids dominated by liquid CO_2.

3.2 Microprofiles

In situ microprofiles of pH, oxygen, sulfide, redox potential and temperature at three different sites were measured in 2008 (Fig. 2a–c) and at two sites in 2010 (Fig. 2d and e). The distances of the five profile sites from the Abyss Vent were 0.5 m, 10 m, 100 m, 125 m and 0.5 km (the reference site). The oxygen sensors were damaged before the measurements at 0.5 m and 100 m, all other microprofile measurements were successful. The oxygen concentrations in the bottom water, measured with in situ sensors and on retrieved water samples in 2008 and 2010, were approximately 0.08 mM at all sites. The reference site showed an oxygen penetration into the sediments of 8 mm. No significant decrease in pH was measured, sulfide was absent, and the redox potential and temperature remained that of the bottom water in the upper 12 cm (Fig. 2e).
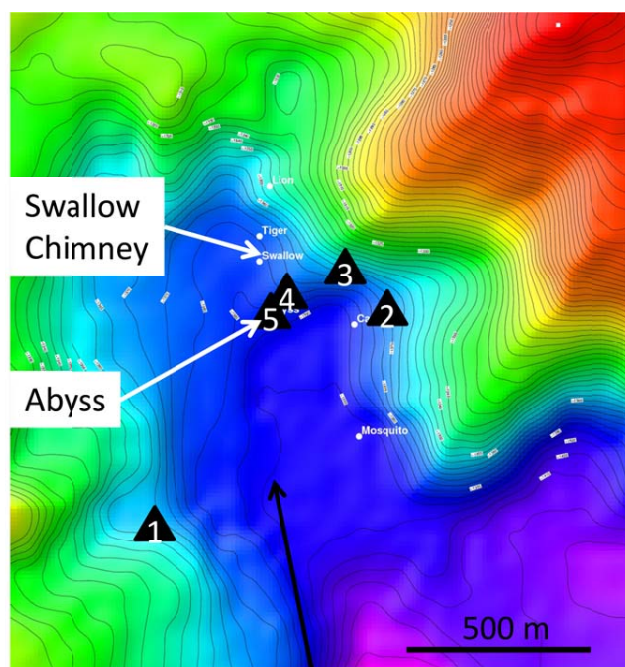
Fig. 1. Bathymetric map of the working area. The microprofiler locations are indicated, at 550 m (1, Reference, MP1 2010), 125 m (2, MP2 2010), 100 m (3, MP3 2008), 10 m (4, MP1 2008) and 0.5 m (5, MP2 2008) distance from Abyss Vent. The black arrow indicates the main bottom water current direction.

The sites closer to the vent showed increasing effects of fluid advection. The oxygen penetration decreased to 5 mm at the site of 125 m distance from the vent (Fig. 2d) and 1 mm at < 10 m distance (Fig. 2b). Sulfide was detected in sediments at 100 m distance (Fig. 2d), and the sulfide profiles became increasingly steeper closer to the vent. Remarkably, they were almost perfectly linear, indicating high transport rates, but relatively low sulfide production in the upper 5 cm. The sediment redox potential decreased rapidly to negative values at the sites closer than 100 m from the vent. The CO_2 sensors showed a drastic increase in signal with depth, surpassing the calibration range of the sensors at < 1 cm depth, and hence could not be used for quantification of CO_2 concentrations. The pH profiles became steeper close to the vent, showing a pH of $\sim 4.5 > 6$ cm below the seafloor (cm b.s.f.) at sites closer than 100 m from the vent. Accordingly, the fluxes of oxygen and sulfide increased when approaching the vents (Table 2). At the site 10 m from the Abyss Vent, the diffusive oxygen flux was almost ten times the sulfide flux. Thus other electron donors than sulfide are needed to explain the high oxygen consumption rate in the sediments.

3.3 Geochemistry

Generally, the porewater profiles were surprisingly heterogeneous, indicating a complex spatial scaling of subsurface transport of hydrothermal fluids and liquid CO_2, as well as intense reactions with the surface sediments. Porewater profiles showed elevated concentrations of sulfide, methane, ammonium (Figs. 3 and 4), manganese and iron (not shown), which may serve as electron donors for microbial oxygen consumption and could explain the enhanced oxygen fluxes in vented sediments. The subsurface porewater retrieved from the vents showed increased concentrations of methane compared to the background site (> 1 mM, 3 out of 5 sites sampled) and sulfide (> 2 mM), but these could not be quantified with precision due to the vigorous degassing upon retrieval on deck. This outgassing was mainly driven by the strong supersaturation of CO_2 and often continued for 10 to 20 minutes after arrival on deck. The loss of CO_2 during retrieval increased the pH to 6 or 7 in the sediments.

Beyond high gas content and elevated concentrations of reduced compounds, the geochemistry showed further substantial effects of CO_2 leakage and hydrothermalism in sediments retrieved close to the vent sites (Figs. 3 and 4). These included steep porewater profiles and high total alkalinity (> 60 meq L^{-1}), low sulfate, and elevated concentrations of silicate (Figs. 3 and 4). Since the sediments around the Swallow Chimney were extensively covered with volcanic rock debris and chimney material, sediment samples could only be recovered by gravity coring. The collected porewaters exhibited also very high total alkalinity and NH_4^+, elevated sulfide, dissolved silicate and methane (Fig. 5). Accordingly, benthic chamber incubations recorded effluxes of ammonium, methane, DIC and silicate near the vents. None of the sites investigated leaked sulfide to the overlying bottom water.

3.4 Microbial respiration rates

The benthic chamber measurements showed rather low total oxygen consumption rates at and near the vent sites which were, however, higher than at the reference site (Table 3). Similar to porewater geochemistry, the rates of sulfate reduction and anaerobic methane oxidation were found to be highly heterogeneous (Fig. 6, standard deviations are not shown for clarity). Areal rates in cores, taken less than 40 cm apart, could differ an order of magnitude in SR and AOM rates. Consequently, areal quantification was not possible based on our sparse coring, but trends can be seen. Generally, both SR and AOM rates were higher close to the vents than at the distant sites > 20 m away, and hence constituents of the hydrothermal fluids fuelled these microbial processes, even under the conditions of high CO_2 concentrations and low pH associated with the vents. However, measurable rates of SR and AOM were limited to the upper 7–15 cm in retrieved cores (Fig. 6a and b). Accordingly, AOM or SR were below detection level in gravity cores from Swallow

Table 2. Fluxes of oxygen and sulfide near the sediment–water interface, calculated from the microprofiles using Fick's law of diffusion, the average integrated areal SR and AOM measured in MUC and PC taken in and near seeps, and fluxes of methane and DIC measured with the benthic chambers. The distances are between the microprofiler and the Abyss Vent. The station code is given in parentheses (see Table 1).

	Areal rates and fluxes ($mol\,m^{-2}\,s^{-1}$)					
Distance to Abyss Vent:	O_2	Sulfide	SR	AOM	CH_4	DIC
Reference 500 m (MP1 2010)	-2×10^{-8}	0	0.05×10^{-8}	0	0	n.d.
125 m (MP2 2010)	-2.3×10^{-8}	0	n.d.	n.d.	n.d	n.d.
100 m (MP3 2008)	#	1.6×10^{-8}	0.15×10^{-8}	0	0.6×10^{-8}	115×10^{-8}
10 m (MP1 2008)	-2.1×10^{-7}	3.5×10^{-8}	n.d.	n.d.	0.1×10^{-8}	30×10^{-8}
0.5 m (MP2 2008)	#	5.8×10^{-8}	6×10^{-8} $(2 \times 10^{-8})^*$	0.1×10^{-8}	4.6×10^{-8}	300×10^{-8}

* Disregarding one outlier rate obtained from MUC10.
n.d. = not determined.
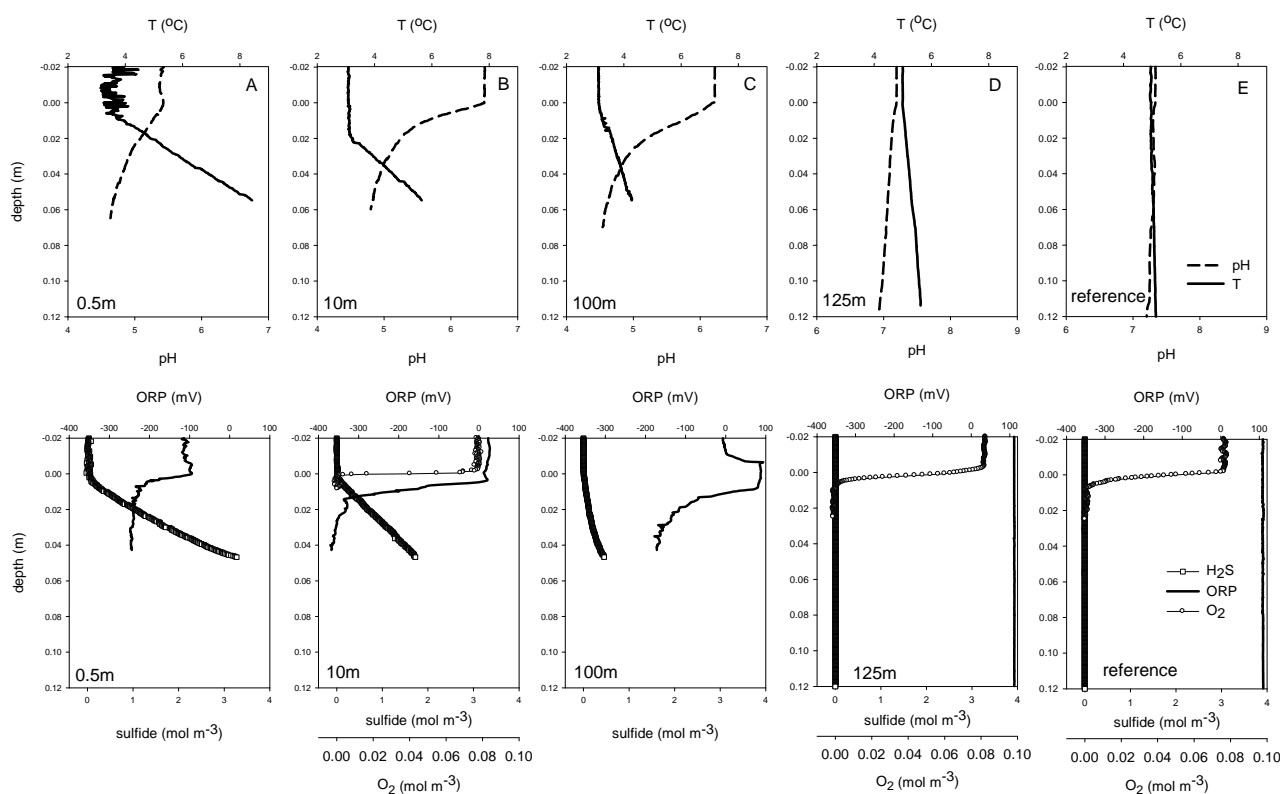
Fig. 2. In situ microprofiles of oxygen, pH, sulfide, ORP (redox potential) and temperature, measured during two cruises in 2008 **(a–c)** and in 2010 **(d)** and **(e)**, at different distances to Abyss Vent. The distances are indicated in the plots; the reference was taken approximately 1 km southwest of the vents. The positions can be found in Table 1. All gradients clearly increase towards the vent.

Chimney, which were sampled in 50 cm intervals, starting at 50 cm b.s.f. (data not shown). Integrated SR rates were on average 6.6×10^{-8} ($\pm 8 \times 10^{-8}$) $mol\,m^{-2}\,s^{-1}$ for sites with high CO_2 leakage (reaching $60\,meq\,L^{-1}$ total alkalinity in > 15 cm sediment depth) around the Abyss Vent and Swallow Chimney, 0.15×10^{-8} ($\pm 0.16 \times 10^{-8}$) $mol\,m^{-2}\,s^{-1}$ for the sites with low CO_2 leakage, and negligible at the reference site. The average of all areal rates of AOM was 0.8×10^{-8} ($\pm 0.2 \times 10^{-8}$) $mol\,m^{-2}\,s^{-1}$ in CO_2 vented sediments near seeps, thus almost a magnitude lower than the SR rates. AOM rates were below the detection limit away from the vents and at the reference site. This suggests that most SR is driven by electron-donors other than methane, indeed H_2 was found in the vent fluids and sediments. The sulfide fluxes, measured with microsensors (Table 2), were much higher than the areal SR rates, indicating that most of
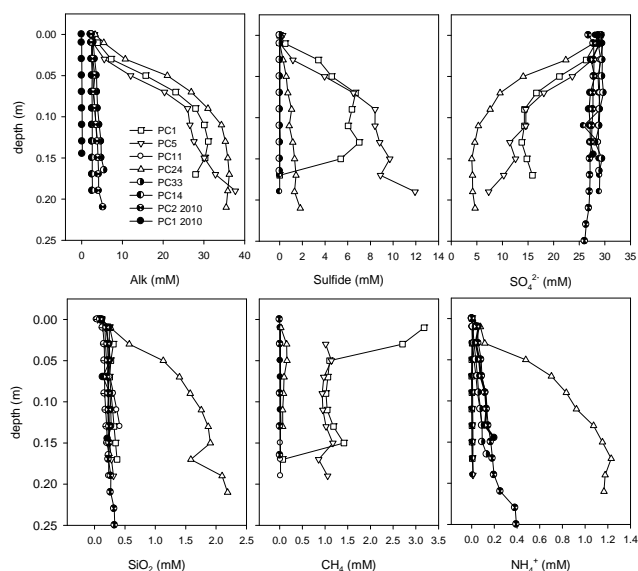
Fig. 3. Porewater chemistry profiles obtained from sediments retrieved by the push cores (PC). The reference data, obtained from a core approximately 550 m southwest of the vents, are indicated with black symbols. Other distances from the Abyss Vent: PC1 (1 m), PC5 (1 m), PC11 (10 m), PC33 (0.5 m), PC24 (2 m), PC14 (10 m), and PC1 2010 (100 m).
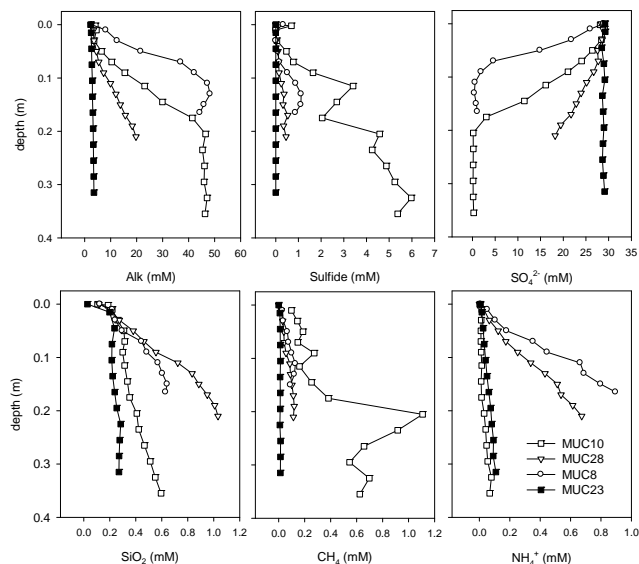
Fig. 4. Porewater chemistry profiles obtained from sediments retrieved by the multicorer (MUC). The positions are given in Table 1. The data from the reference site, approximately 550 m southwest of the vents, are indicated with black symbols. The other cores are from the Abyss Vent area. MUC 10 is the only core among all sediments sampled that showed sulfate depletion.

the sulfide diffusing to the sediment surface does not originate from SR in the upper sediments, but was transported with hydrothermal fluids. Indeed, the highest sulfide concentration was found in a deep GC core (GC1) with clear hydrothermal signatures, such as high dissolved silica and ammonium concentrations (Fig. 5).

4   Discussion

We observed a large heterogeneity of the porewater geochemistry and rates of microbial activity, suggesting complex transport processes of CO_2 in this area. CO_2 is transported in its supercritical form from hot subsurface strata to the cooler surface seafloor where it liquefies and CO_2 hydrates may form (Konno et al., 2006). Spontaneous release of liquid CO_2 was observed from the rocky vent chimneys, but rarely from the sedimentary seafloor. Here, emission of liquid CO_2 was induced only upon disturbance of the surface seabed, e.g. by penetrating the top 20 cm with a temperature probe or with coring gear. The heterogeneity of the geochemistry can partially be understood from the different phases in the sediments. The density of pure liquid CO_2 (Span and Wagner, 1996) is approximately $100\,\mathrm{kg\,m^{-3}}$ lower than that of CO_2-saturated surrounding porewater ($1050\,\mathrm{kg\,m^{-3}}$; (Duan et al., 2008), whereas the CO_2 hydrates on the shallow seafloor have a higher density; thus the system is unstable. Supercritical and liquid CO_2 may finger upwards through the sediments, and may tend to creep inside the sediments from the
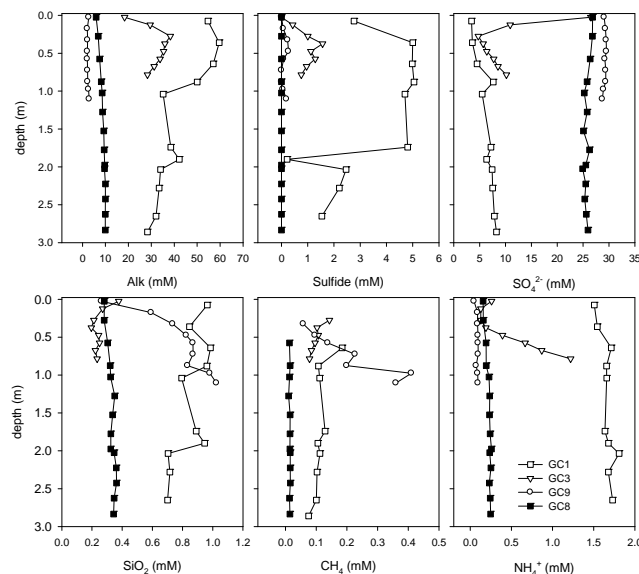
Fig. 5. Porewater chemistry profiles obtained from sediments retrieved by the gravity corer (GC). The data from the reference core (GC 8), taken approximately 1 km southwest of the vents, are indicated with black symbols. GC 9 was obtained 50 m south of Abyss Vent; GC 1 and 3 were taken near the Swallow Chimney.

subsurface hydrothermal reservoirs laterally through the valley (Inagaki et al., 2006). Depending on heat gradients, its seepage is inhibited by gas hydrate formation and the high viscosity of the liquefied CO_2 (Fenghour et al., 1998).
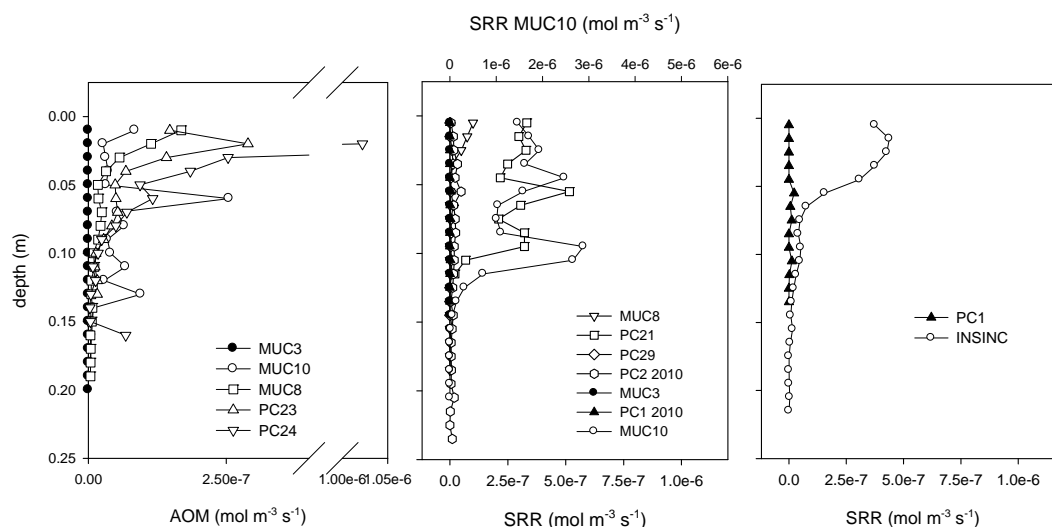
Fig. 6. Microbial rates. **(A)** AOM rates measured on retrieved cores. Although the scatter was large and rates low despite relatively high methane and sulfate concentrations, AOM activity was detectable in the upper 7 cm. **(B)** The SR rates measured on retrieved cores. Values from MUC10 were very high and therefore plotted on a separate x axis above the graph. The SR activities are restricted to the upper 10–13 cm. **(C)** In situ measured SR rates show only significant activities above 7 cm b.s.f. The black symbols represent measurements at the reference site.

In situ, at pressures of > 130 atm, dissolved CO$_2$ concentrations in equilibrium with CO$_2$ hydrate, liquid, or supercritical CO$_2$ may reach 1000–1700 mM (Duan and Sun, 2003; Duan et al., 2006). We estimate that these concentrations are reached at about 20 cm depth, corresponding to our in situ flux measurement by benthic chamber of 300×10^{-8} mol m^{-2} s^{-1}. This flux can be explained by diffusion alone, as the calculated diffusive fluxes range from 200–400×10^{-8} mol m^{-2} s^{-1}, assuming a diffusion distance of 0.2–0.3 m, an effective diffusion coefficient of 0.6–0.8×10^{-9} m^2 s^{-1} at the porosity of 0.7 at 1380 m water depth, and a temperature of 5–15 °C. However, fluid convection cells will develop in sediments very close to the seeps, where upward flow close to the hot seeps is compensated by inflow of seawater at some distance around the seeps. The diameter of such cells is thought to be a few metres (Haeckel and Wallmann, 2008). As a result of the complex transport phenomena, the porewater composition is highly variable between vents and seeping sediment sites.

The fluxes of DIC, methane and ammonium far exceed the oxygen uptake, the SR and the AOM rates. Thus, microbiological processes hardly influence the geochemistry of the vented sediments. Despite the local variability of heat, fluid, CO$_2$ and energy transport, it is obvious that CO$_2$ leakage around the vent systems reduces the pH of the sedimentary environment. The enhanced alkalinity and silicate concentrations are due to weathering of silicates:

$$MeSiO_3 + H_2O + 2H^+ \rightarrow Me^{2+} + H_4SiO_4, \tag{1}$$
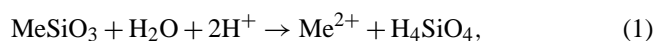
where Me can be Ca^{2+} or Mg^{2+}. The reaction leads to a pH increase, and thus shifts the carbonate equilibrium away from

CO$_2$, as is clear from a more general formulation (Wallmann et al., 2008):

$$\text{reactive silicates} + CO_2 \rightarrow \text{metal cations} \tag{2}$$
$$+ \text{dissolved silica} + HCO_3^-.$$
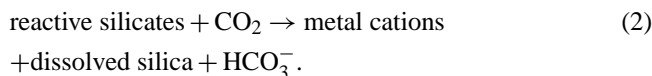
As dissolved CO$_2$ is indirectly a substrate, this process will be drastically enhanced at the extremely high CO$_2$ levels at the vented sites, as confirmed by the high subsurface concentrations of SiO$_2$. Thus the sequestration of liquid CO$_2$ in the deep seabed will indeed lead to enhanced weathering of the sediments, and consumption of protons. However, this practice will also lead locally to strong ecosystem effects. We will further discuss the most severe consequences for microbial life and element cycling.

CO$_2$-enriched hydrothermal fluids of Yonaguni Knoll IV co-migrate from large depth with CH$_4$, H$_2$S and NH$_3$ and H$_2$ (Konno et al., 2006). The concentrations of H$_2$ and CH$_4$ in the hydrothermal fluids vary between 1 and 10 mM. These potential electron donors for microbial reactions are products of mainly thermal degradation of organic matter. When reaching the cooler, oxidized seawater, the high fluxes of reduced compounds could drive a suite of metabolic activities, usually known to turn hydrothermal vents and cold seeps to oases of life, attracting numerous types of chemosynthetic bacteria. However, at the Yonaguni Knoll IV site chemosynthesis seems limited to the chimneys. Microbial mats that are characteristic for highly productive sediments were absent. Generally, microbial life is very limited in the vented sediments. Notably, with $\sim 5 \times 10^{-8}$ mol, oxygen consumption (Table 3) appeared substantially repressed compared to that of other seeps and vents with similar concentrations

Table 3. In situ fluxes obtained from the benthic chambers near Abyss Vent.

Distance to vent:	O_2 (mol m^{-2} s^{-1})	CH_4 (mol m^{-2} s^{-1})	DIC (mol m^{-2} s^{-1})	Si (mol m^{-2} s^{-1})	NH_3 (mol m^{-2} s^{-1})	Dive, chamber number
Reference 500 m	-0.9×10^{-8}	0	n.d.	0	0	206, 1
25 m	-4.6×10^{-8}	0.6×10^{-8}	115×10^{-8}	52×10^{-8}	0.7×10^{-8}	206, 2
10 m	n.d.	0.07×10^{-8}	30×10^{-8}	5.8×10^{-8}	5.8×10^{-8}	203, 1
0.5 m	-4.6×10^{-8}	4.6×10^{-8}	300×10^{-8}	14×10^{-8}	12×10^{-8}	203, 2

n.d. = not determined.

of reduced compounds in surface porewaters (Felden et al., 2010; Ristova et al., 2012). Typically, methane seeps at similar water depths show oxygen consumption rates of 10–100×10^{-8} mol.

Furthermore, the interfacial fluxes of sulfide were almost always much higher than the integrated SR rates (with exception of the rates measured in MUC10), thus most of the emitted sulfide originates from hydrothermal processes, and microbial production by SR was only a small fraction of the sulfide budget. This is also clear from the almost linear sulfide profiles, indicating the dominance of transport and the absence of significant sulfide conversions. Interestingly, both sulfate and methane were consistently present in the sediments, even at larger depths (Fig. 5), and H_2 was present in the vent fluids and sediments (Konno et al., 2006), but no sulfate reduction was detected below 15 cm depth (Fig. 6). Only relatively low SR and AOM rates were measured at the vents, as compared to other methane-rich hydrothermal vents and seeps that are not impacted by CO_2 leakage (Biddle et al., 2011; Felden et al., 2010).

Hence, an important question is as to what restricts microbial anaerobic respiration to the upper 7–15 cm layer, despite the availability of chemical energy. Experiments carried out with marine sediments showed the potential for SR up to temperatures of 60 °C (Holler et al., 2011). From extrapolation of the interfacial gradients based on the temperature profiles measured with the microprofiler, we estimate that 60 °C is reached at 2.5 m, 0.8 m and 0.6 m b.s.f. at the locations 100 m, 10 m and 0.5 m from the Abyss Vent. This indicates that lethal temperatures are only reached far below the upper 15 cm depth horizons and should not limit microbial activity here. Then, possibly, the low pH might constrain AOM and SR. However, shore-based incubation experiments with sediments from the same site showed that SR was not inhibited at a pH value of 4.5 or even at pH 3 (Yanagawa et al., 2012). An essential difference between these ex situ incubation experiments with rate measurements under in situ conditions are the CO_2 levels to which the microbial communities are exposed. It should be noted that at the low ambient pH, well below the pK_1, almost all DIC will be in the form of CO_2. The in situ dissolved CO_2 concentrations of

1000–1700 mM far exceed the ~ 30 mM that can be reached in CO_2-saturated seawater at 1 atm.

Liquid and supercritical CO_2 are highly powerful apolar solvents that will disintegrate cytoplasmic membranes, and thus are lethal for all life forms. Droplets of liquid CO_2 were consistently observed upon retraction of push cores by the ROV arm around the Abyss Vent, indicating that liquid CO_2 reached to 20–30 cm b.s.f. In the deeper sediments, where temperature exceeded the critical point of CO_2 (i.e. 31 °C), supercritical CO_2 was present. However, the liquid and supercritical CO_2 only occupy a fraction of the pore space, as many ionic species were found in concentrations common for seawater. CO_2 may be unevenly present in the form of droplets or bubbles that are retained in the low-permeability hydrothermal sediments. However, also in the porewater near liquid and/or supercritical CO_2, most life will be unlikely. AOM, with its very low energy yield, will not be possible due to end-product inhibition. As H_2 is present in vent fluids and sediments, sulfate reduction was expected wherever sulfate is present. However, sulfate reduction did not occur. The extremely high levels of CO_2 will be toxic for most forms of life, as it will pass the membranes, dissipate the ΔpH across the cell membrane, and thus disrupt the cellular pH homeostasis. Most microbes need to maintain a near neutral cytoplasmic pH, and do so even under the most extreme external pH levels. Thus cytoplasm acidification will inhibit most microbial activity at pH 4.5 and 1700 mM CO_2. The stalling of biogeochemical processes in deep-sea CO_2 seeps and disposal areas will have drastic consequences for the local ecosystem. The current understanding of physiological adaptation strategies to high CO_2 and of overall ecological consequences of CO_2 leakage for seafloor ecosystems is still limited; however, our observations at the Yonaguni natural CO_2 vents suggest that the liquid or supercritical CO_2 reservoirs could form one of the harshest environments for life as we know it. It may well be that microbial cells and preserved DNA and RNA are found in such extremely CO_2-rich habitats. These cells will be, however, inactive or dead. Further experimental work will be needed for testing the physiological effects of extremely high CO_2 levels on pH homeostasis, using high-pressure reactors.

Edited by: G. Herndl

References

Biddle, J. F., Cardman, Z., Mendlovitz, H., Albert, D. B., Lloyd, K. G., Boetius, A., and Teske, A.: Anaerobic oxidation of methane at different temperature regimes in Guaymas Basin hydrothermal sediments, ISME J., 6, 1018–1031, 2011.

de Beer, D., Schramm, A., Santegoeds, C. M., and Kühl, M.: A nitrite microsensor for profiling environmental biofilms, Appl. Environ. Microbiol., 63, 973–977, 1997.

Duan, Z. and Sun, R.: An improved model calculating CO_2 solubility in pure water and aqueous NaCl solutions from 273 to 533 K and from 0 to 2000 bar, Chem. Geol., 193, 257–271, 2003.

Duan, Z., Sun, R., Zhu, C., and Chou, I.-M.: An improved model for the calculation of CO_2 solubility in aqueous solutions containing Na^+, K^+, Ca^{2+}, Mg^{2+}, Cl^-, and SO_4^{2-}, Mar. Chem., 98, 131–139, 2006.

Duan, Z., Hu, J., Li, D., and Mao, S.: Densities of the CO_2-H_2O and CO_2-H_2O-NaCl systems up to 647 K and 100 MPa, Energ. Fuel., 22, 1666–1674, 2008.

Felden, J., Wenzhoefer, F., Feseker, T., and Boetius, A.: Transport and consumption of oxygen and methane in different habitats of the Hakon Mosby Mud Volcano (HMMV), Limnol. Oceanogr., 55, 2366–2380, 2010.

Fenghour, A., Wakeham, W. A., and Vesovic, V.: The viscosity of carbon dioxide, J. Phys. Chem. Ref. Data, 27, 31–44, 1998.

Grasshoff, K., Kremling, K., and Ehrhardt, M.: Methods of Seawater Analysis, Wiley, Weinheim, 600 pp., 1999.

Gundersen, J. K. and Jørgensen, B. B.: Microstructure of diffusive boundary layers and the oxygen uptake of the sea floor, Nature, 345, 604–607, 1990.

Haeckel, M. and Wallmann, K.: Indications for convective flow induced by focussed fluid venting at bacterial mats, Geochim. Cosmochim. Ac., 72, A340–A405, 2008.

Holler, T., Widdel, F., Knittel, K., Amann, R., Kellerman, M. Y., Hinrichs, K. U., Teske, A., Boetius, A., and Wegener, G.: Thermophilic anaerobic oxidation of methane by marine microbial consortia, ISME J., 5, 1946–1956, 2011.

House, K. Z., Schrag, D. P., Harvey, C. F., and Lackner, K. S.: Permanent carbon dioxide storage in deep-sea sediments, P. Natl. Acad. Sci., 103, 12291–12295, 2006.

Inagaki, F., Kuypers, M. M. M., Tsunogai, U., Ishibashi, J., Nakamura, K., Treude, T., Ohkubo, S., Nakaseama, M., Gena, K., Chiba, H., Hirayama, H., Nunoura, T., Takai, K., Joergensen, B. B., Horikoshi, K., and Boetius, A.: Microbial community in a sediment-hosted CO_2 lake of the southern Okinawa trough hydrothermal system, P. Natl. Acad. Sci, 103, 14164–14169, 2006.

IPCC: Contribution of Working Group I to the Fourth Assessment Report of the Intergovernmental Panel on Climate Change, Cambridge University Press, Cambridge, United Kingdom and New York, NY, USA, 996, 2007.

Jeroschewski, P., Steukart, C., and Kühl, M.: An amperometric microsensor for the determination of H_2S in aquatic environments., Anal. Chem., 68, 4351–4357, 1996.

Jørgensen, B. B. and Boetius, A.: Feast and famine – microbial life in the deep-sea bed, Nat. Rev. Microbiol., 5, 770–781, 2007.

Jørgensen, B. B. and Nelson, D. C.: Sulfide oxidation in marine sediments: geochemistry meets microbiology, Geol. Soc. Am., 379, 63–81, 2004.

Konno, U., Tsunogai, U., Nakagawa, F., Nakaseama, M., Ishibashi, J., Nunoura, T., and Nakamura, K.: Liquid CO_2 venting on the seafloor: Yonaguni Knoll IV hydrothermal system, Okinawa Trough, Geophys. Res. Lett., 33, L16607, doi:10.1029/2006GL026115, 2006.

Liu, J., Weinbauer, M. G., Maier, C., Dai, M., and Gattuso, J. P.: Effect of ocean acidification on microbial diversity and on microbe-driven biogeochemistry and ecosystem functioning, Aquat. Microb. Ecol., 61, 291–305, 2010.

Millero, F. J., Plese, T., and Fernandez, M.: The dissociation of hydrogen sulfide in seawater., Limnol. Oceanogr., 33, 269–274, 1988.

Nunoura, T., Oida, H., Nakaseama, M., Kosaka, A., Ohkubo, S. B., and Kikuchi, T.: Archaeal diversity and distribution along thermal and geochemical gradients in hydrothermal sediments at the Yonaguni Knoll IV hydrothermal field in the Southern Okinawa Trough, Appl. Environ. Microbiol., 76, 1198–1211, 2010.

Reeburgh, W. S.: Rates of biogeochemical processes in anoxic sediments, Annu. Rev. Earth Planet Sci., 11, 269–298, 1983.

Rehder, G. and Schneider von Deimling, J.: RV Sonne Cruise Report SO 196 SUMSUN 2008, 71, 2008.

Revsbech, N. P.: An oxygen microelectrode with a guard cathode, Limnol. Oceanogr., 55, 1907–1910, 1989.

Sakai, H., Gamo, T., Kim, E. S., Tsutsumi, M., Tanaka, T., and Ishibashi, J.: Venting of carbon dioxide-rich fluid and hydrate formation in mid-Okinawa trough backarc basin, Science, 248, 1093–1096, 1990.

Seibel, B. A. and Walsh, P. J.: Potential Impacts of CO_2 Injection on Deep-Sea Biota, Science, 294, 319–320, 2001.

Sibuet, J. C., Letouzey, J., Barbier, F., Charvet, J., Foucher, J. P., and Hilde, T. W. C.: Back arc extension in the Okinawa Trough, J. Geophys. Res., 92, 14041–14063, 1987.

Span, R. and Wagner, W.: A new equation of state for carbon dioxide covering the fluid region from the triple-point temperature to 1100K at pressures upto 800 MPa, J. Phys. Chem. Ref. Data, 25, 1509–1596, 1996.

Stan-Lotter, H. and Fendrihan, S.: Adaption of Microbial Life to Environmental Extremes, Novel Research Results and Applica-

tion, Springer, Vienna, New York, 282 pp., 2012.

Suzuki, R., Ishibashi, J. I., Nakaseama, M., Konno, U., Tsunogai, U., Gena, K., and Chiba, H.: Diverse Range of Mineralization Induced by Phase Separation of Hydrothermal Fluid: Case Study of the Yonaguni Knoll IV Hydrothermal Field in the Okinawa Trough Back-Arc Basin, Resource Geol., 58, 267–288, 2008.

Treude, T., Krüger, M., Boetius, A., and Jørgensen, B. B.: Environmental control on anaerobic oxidation of methane in the gassy sediments of Eckenfoerde Bay (German Baltic), Limnol. Oceanogr., 50, 1771–1786, 2005.

Wallmann, K., Aloisi, G., Haeckel, M., Tishchenko, P., Pavlova, G., and Greinert, J.: Silicate weathering in anoxic marine sediments, Geoch.Cosmoc.Acta, 72, 2895–2918, 2008.

Yanagawa, K., Morono, Y., De Beer, D., Haeckel, M., Sunamura, M., Futigami, T., Hoshino, T., Terada, H., Nakamura, K. I., Urabe, T., Rehder, G., Boetius, A., and Inagaki, F.: Metabolically active microbial communities in marine sediment under high-CO$_2$ and low-pH extremes, ISME J., 7, 555–567, 2012.